Experimental Neurology **169,** 340–350 (2001)
doi:10.1006/exnr.2000.7626, available online at http://www.idealibrary.com on IDEAL®

Early Degenerative Changes in Transgenic Mice Expressing Mutant Huntingtin Involve Dendritic Abnormalities but No Impairment of Mitochondrial Energy Production

Paolo Guidetti,*,[1] Vinod Charles,†,[1] Er-Yun Chen,‡ P. Hemachandra Reddy,† Jeffrey H. Kordower,‡ William O. Whetsell, Jr.,§ Robert Schwarcz,* and Danilo A. Tagle†,[2]

*†National Human Genome Research Institute, NIH, 49 Convent Drive, Bethesda, Maryland 20892; *Maryland Psychiatric Research Center, University of Maryland School of Medicine, Baltimore, Maryland 21228; ‡Research Center for Brain Repair, Rush Medical School, Chicago, Illinois 60612; and §Vanderbilt University School of Medicine, Nashville, Tennessee 37232*

Received October 17, 2000; accepted December 19, 2000

Mitochondrial defects, which occur in the brain of late-stage Huntington's disease (HD) patients, have been proposed to underlie the selective neuronal loss in the disease. To shed light on the possible role of mitochondrial energy impairment in the early phases of HD pathophysiology, we carried out Golgi impregnation and quantitative histochemical/biochemical studies in HD full-length cDNA transgenic mice that were symptomatic but had not developed to a stage in which neuronal loss could be documented. Golgi staining showed morphologic abnormalities that included a significant decrease in the number of dendritic spines and a thickening of proximal dendrites in striatal and cortical neurons. In contrast, measurements of mitochondrial electron transport Complexes I–IV did not reveal changes in the striatum and cerebral cortex in these mice. Examination of the neostriatum and cerebral cortex in human presymptomatic and pathological Grade 1 HD cases also showed no change in the activity of mitochondrial Complexes I–IV. These data suggest that dendritic alterations precede irreversible cell loss in HD, and that mitochondrial energy impairment is a consequence, rather than a cause, of early neuropathological changes. © 2001 Academic Press

Key Words: **mitochondrial; Huntington's; Golgi; neurodegeneration; transgenic; mouse; dendrites; striatum.**

INTRODUCTION

Huntington's disease (HD) is an adult-onset, dominantly inherited neurodegenerative disorder characterized by involuntary choreiform movements, cognitive impairment and other behavioral abnormalities (18). The neuropathological hallmarks of HD include preferential loss of striatal medium spiny neurons and cortical pyramidal cells, but behavioral impairment in HD patients can occur with little or no evidence of neurodegeneration (72). The genetic defect in HD lies in the expansion of tandem polyglutamine repeats in the huntingtin protein (31). However, since huntingtin is widely distributed in neurons and peripheral cells (44, 65, 67), it is unclear how the mutation causes the distinct behavioral changes and the selective neuronal loss seen in HD (57).

In studies using transgenic mice expressing full-length mutant huntingtin, we recently demonstrated that progressive behavioral and locomotor abnormalities began as early as 2 months of age, whereas neuronal loss and astrocytosis were not apparent until much later (56, 57). We speculated that the animals' early phenotype presentation might be related to malfunctioning neurons and, more specifically, that early functional impairment might involve irregular synaptic transmission and/or bioenergetic deficits (55–57).

Abnormalities in mitochondrial enzyme activities have been demonstrated in several neurodegenerative diseases including HD (13–15, 24, 25, 51, 68) and have been repeatedly suggested to play an early and principal role in the cascade of events that ultimately result in irreversible neuronal damage (8, 60). Mitochondrial oxidative phosphorylation is the major source of ATP in aerobic organisms and consists of an integrated system of protein complexes (NADH ubiquinone oxidoreductase or Complex I; succinate ubiquinol oxidoreductase or II; ubiquinol cytochrome c oxidoreductase or III; and cytochrome c oxidase or IV) located in the mitochondrial inner membrane. These complexes act as two series of enzymes (Complexes I, III, and IV or Complexes II, III, and IV) to oxidize NADH and $FADH_2$ through an electron transport chain that ulti-

[1] These authors contributed equally to this work.

[2] To whom correspondence should be addressed at Building 49, Room 3A26, 49 Convent Drive, Bethesda, MD 20892. Fax: (301) 402-4929. E-mail: datagle@helix.nih.gov.

0014-4886/01 $35.00

mately leads to the terminal electron acceptor ATP synthase. Impairment of the electron transfer chain is believed to disrupt ATPase-dependent Na^+–K^+ membrane pumps which in turn impedes the neuron's ability to maintain a normal resting potential and eventually causes cell death. In support of this hypothesis, experimentally induced reductions in mitochondrial energy metabolism, caused for example by compounds such as 3-nitropropionate, malonate, or azide, increase vulnerability to excitotoxic insults or produce excitotoxic damage on their own (9, 10, 23, 24, 35, 76, 77). Notably, intrastriatal injections of these compounds in animals have been used to provide valuable HD models (7, 24).

The present study was designed to examine the possible role of respiratory chain abnormalities in the early phases of HD pathophysiology. In particular, we measured the activities of the four mitochondrial complexes in HD full-length cDNA transgenic mice expressing mutant huntingtin with either 48 or 89 polyglutamines ("HD48" and "HD89") and in age-matched wild-type mice. In separate animals, Golgi staining was employed to identify possible morphological changes in striatal and cortical neurons. All mice used in the study were initially characterized with regard to their behavioral phenotype. Finally, we examined the activity of the respiratory chain enzymes in presymptomatic and early symptomatic human HD cases and compared the results with those obtained from late-stage HD cases.

MATERIALS AND METHODS

Materials

Nicotinamide adenine dinucleotide (reduced form; NADH), succinic acid, cytochrome c, 3,3′-diaminobenzidine, nitroblue tetrazolium, ubiquinone 1, and ubiquinone 2 were obtained from Sigma Chemical Co. (St. Louis, MO). All other chemicals were purchased from different commercial suppliers and were of the highest available purity.

Animals

Wild-type mice (FVB/N strain, Taconic, Germantown, NY) and heterozygous transgenic mice expressing full-length huntingtin (bred on a FVB/N background) (56) were housed in an AAALAC-approved animal facility in accordance with institutional guidelines. The animals were kept on a 12-h/12-h light/dark cycle with free access to food and water.

Human Subjects

Frozen blocks of human tissues [striatum, cerebral cortex (Brodmann areas 5 and 6)] were obtained from the Harvard Brain Tissue Resource Center (McLean Hospital, Boston, MA). The specimens were divided into three groups: (a) presymptomatic HD gene carriers ($n = 2$) and grade 1 ($n = 5$) HD cases (age, 64.6 ± 7.9; postmortem interval (PMI), 12.4 ± 2.4); (b) grade 3 ($n = 1$) and grade 4 ($n = 2$) HD cases (age, 63.7 ± 3.7; PMI, 18.9 ± 1.5); (c) 9 controls (age, 65.4 ± 3.3; PMI, 15.2 ± 1.6). DNA was extracted and used for genotype analysis using previously published procedures (71). The mutant alleles in the HD cases ranged from 45 to 50 CAG repeats.

Behavioral Analyses

Mice (HD 48 $n = 9$, HD 89 $n = 10$, wild-type $n = 5$) were first tested for changes in locomotor activity and coordination. Gross neurological evaluation of mice for spontaneous behaviors, tail-suspension immobility, feet clasping, excessive grooming, and general appearance revealed qualitative differences between HD transgenics and wild-type controls (data not shown). Mice were analyzed once per week for 3 weeks using an open-field activity monitor (Benwick Electronics) to assess changes in locomotor activity, as measured by the frequency of photobeam breaks over a 5-min interval. Differences in locomotor activity between transgenic and wild-type mice as indicated by percentage mobility (overall motor activity when the animal is moving) was measured.

HD transgenic and wild-type animals were also tested for deficits in motor coordination using a rotarod apparatus (IITC, Inc., Life Instruments), with a maximum latency of 30 s. Three trials were performed at a fixed speed of 5.0 rpm with a 5-min interval between trials. The first trial was intended to be a habituation run and only the means of the second and third trials were used for each animal. These mice were used subsequently for evaluation of mitochondrial energy impairment and for stereological assessment of striatal neurons.

Tissue Preparation

Animals were sacrificed, and the extracted brain was flash-frozen in cooled isopentane and stored at −80°C. Serial 12-μm (mice) or 30-μm (human) sections were cut at −20°C using a cryostat. Every 25th section of the mouse striatum and every 10th section of the human cortex and neostriatum were collected on polylysine-coated slides and stored at −80°C until staining. For Golgi impregnation studies, brains were immersed and stored in 10% formalin.

Immunocytochemistry

One series of sections from each brain was processed for immunohistochemical visualization of the neuronal marker neuronal nuclear antigen (NeuN) via the biotin-labeled antibody procedure. Briefly, the sections

were fixed by immersion in 4% paraformaldehyde in 0.1 M sodium phosphate buffer (PBS) for 10 min. Sections were then rinsed with phosphate-buffered saline (PBS) for 5 min. Following several washes in Tris-buffered saline (TBS) solution containing 0.1% Triton X-100 (TBS-TX), sections were incubated for 20 min in a TBS solution containing 0.5% H_2O_2 to eliminate endogenous peroxidase activity. After three washes in TBS-TX, background staining was inhibited by a 1-h incubation in 5% normal horse serum and 2% bovine serum albumin. The primary antibody (mouse anti-NeuN monoclonal antibody; Chemicon, CA) was then applied overnight (1:1000) at room temperature in 0.1 M PBS containing 0.4% Triton X-100 and 5% normal horse serum. After six washes in TBS-TX, sections were sequentially incubated in biotinylated horse anti-mouse IgG (Vector Labs, Burlingame, CA; 1:200) for 1 h and with the "Elite" avidin–biotin complex (ABC Kits, Vector Labs; 1:500) for 75 min, separated by 3 washes in TBS-TX. The chromogen solution that completed the reaction consisted of 0.05% 3′3-diaminobenzidine (DAB) and 0.005% H_2O_2. Sections were dehydrated through graded alcohol (50, 70, 95, 99%), cleared in xylenes, and coverslipped with Cytoseal.

Stereological Assessment of NeuN-ir Striatal Neurons

Estimation of the total number of striatum containing NeuN immunoreactivity (-ir) neurons was achieved by using the optical fractionator procedure (73, 74). One series of sections from each case comprising 8 to 12 sections was used for analysis. The optical fractionator procedure, a design-based stereological method for estimating the total number of profiles within a structure, uses high-power magnification (100×) with high numerical aperture (na = 1.4) in a known fraction of a defined reference space. Quantification using this method is unaffected by tissue shrinkage or structure volume. Briefly, our optical fractionator system consisted of a computer-assisted image analysis system including an Olympus BX-60 microscope hard-coupled to a Prior H128 computer-controlled $X–Y–Z$ motorized stage, a high-sensitivity Hitachi 3CCD video camera system (Hitachi, Japan), and a Macintosh 8500 computer. The NeuroZoom software (NeuroZoom, La Jolla, CA) performed all analyses. This program automatically records the number of profiles within a structure. The total number of NeuN-ir neurons within the striatum was performed by an observer unaware of the genetic background of the animals. Rough boundaries to delimit the optical fractionator areal sampling were drawn by using a 4× objective. Five percent of the outlined region was measured with a systematic random design of dissector counting frames. After initially focusing on the top of the section, which served as the forbidden plane, a guard focus height of 2 μm was set in the software, which then focused 4 μm through each sample region. The mean thickness of each section was empirically determined to be 7.28 μm. An immunoreactive perikaryon was used as an inclusion criterion. By calculating the total number of raw counts (Q), section sampling fraction (ssf), area sampling fraction (asf), and thickness sampling fraction (h/t), the total number of NeuN-ir neurons of the striatum can be calculated using the formula:

$$N = Q \times 1/\text{ssf} \times 1/\text{asf} \times t/h.$$

Golgi Impregnation

Golgi staining was carried out using a modification of the technique of Landas and Phillips (43). Tissue from HD transgenic and wild-type mice (striatum and sensorimotor cortex) was cut into 4- to 5-mm-thick blocks, rinsed for 20 min in 0.9% NaCl, placed into acid-cleaned plastic cassettes, and immersed in an impregnation solution (5% potassium dichromate:4% potassium chromate:1% mercuric chloride:distilled water, 1:1:1:2) in an acid-cleaned glass flask. The flask was sealed and covered with foil, and the solution was slowly and continuously agitated for 10 days. The tissue blocks were then removed, rinsed thoroughly with water, and immersed for 6 h in an alkalizing solution (0.5 g LiOH and 15.0 g KNO_3 in 100 ml distilled water) in a lighttight glass container. Tissue blocks were then submerged for 18 h in 0.2% glacial acetic acid, washed for 2 h in distilled water, dehydrated in graded alcohol, and embedded in Spurr's epoxy embedding medium. The blocks were then cut into 30-μm sections, which were placed on glass slides, air dried, and coverslipped for light microscopic analyses. Golgi impregnated neurons and processes from mutant HD transgenic mice and wild-type controls were assessed for (changes in) dendritic and somatic morphology. Photomontages (400×) of both striatal and cortical neurons were used for direct counting of dendritic spines along 20-μm lengths of primary and secondary dendrites. The same photomontages were then scanned and imaged using ADOBE Photoshop, and the images were quantified using NIH-Image. Grayscale threshold images, which allow better contrast for edge-type measurements of dendritic spines, were used to measure total neuronal area (μm^2) and the area of four primary dendrites per neuron. Calculations were based on average measurements of 11–15 striatal and 5–15 cortical neurons per experimental group.

Histochemical Procedures

Serial 12-μm (mouse)- or 30-μm (human)-thick sections were cut coronally at −20°C using a cryostat and were collected on polylysine-coated slides and stored at −80°C. Complex I was visualized by incubating the sections at room temperature (22°C) in 200 mM Tris–

HCl buffer, pH 7.4, containing 0.5 mg/ml of both NADH and nitroblue tetrazolium for 20 min (66). Sections were subsequently rinsed in phosphate buffer (PB), pH 7.4, postfixed in 4% neutral-buffered formaldehyde for 10 min, rinsed in water, and coverslipped using Faramount (Dako Co., Carpinteria, CA). Complex II staining was performed by incubating the sections for 10 min in phosphate-buffered saline (PBS), pH 7.4, at 37°C to break tight oxaloacetate bonds (1). Sections were rinsed in PBS, pH 7.4, and subsequently incubated for 25 min at 37°C in PB, pH 7.5, containing 50 mM succinate and 0.5 mg/ml nitroblue tetrazolium (2). Sections were rinsed, postfixed, and coverslipped as described above. Since Complex III cannot be visualized histochemically, the activity of dihydroubiquinone:cytochrome c oxidoreductase was determined biochemically (cf. below). Complex IV staining was accomplished by incubating the sections at 37°C for 30 min (mouse) or 90 min (human) in 100 mM Hepes buffer, pH 7.4, containing 22.4 mg cytochrome c, 115 mg 3,3′-diaminobenzidine, 4.5 g sucrose, and 12.5 ml 1% nickel ammonium phosphate in 100 ml of buffer, as described by Poeggeler *et al.* (54).

Quantitative analyses were performed by an investigator unaware of the sample codes using standards of known activity for each mitochondrial enzyme complex, a video-based image analysis system, and Loats Image Analysis software (Silver Spring, MD). Standard sections at different thicknesses (to mimic different amounts of the enzymes) were used in each incubation. A linearity test was performed for each set of standards to assure correct transformation from optical density to enzyme activity (19, 27).

Spectrophotometric Enzyme Assays

Mouse and human tissue was homogenized by sonication in distilled water (1:5, w/v), and aliquots of the resulting homogenates were further diluted with the appropriate buffer for each of the mitochondrial Complex determinations. Enzyme activities were measured as follows: Complex I, rate of oxidation of NADH at 340 nm in the presence of ubiquinone 1 (30); Complex II, rate of reduction of phenazinemetosulfate by succinate at 600 nm (1); Complex III, rate of reduction of cytochrome c at (550–540 nm) using a reduced form of ubiquinone 2 as a substrate (29); Complex IV, rate of oxidation of cytochrome c at 550 nm (32).

Striatal Quinolinate Lesion in FVB/N Mice

Under chloral hydrate anesthesia (360 mg/kg, ip), 2-month-old wild-type FVB/N mice were mounted in a David Kopf stereotaxic apparatus (Tujunga, CA) with the upper incisor bar set at 2.5 mm below the interaural line. A unilateral intrastriatal injection of quinolinate (60 nmol/0.5 μl) was made over 5 min (A, 1.1 mm anterior to bregma; L, 2.2 mm from the midline; V, 3.1 mm below the dura). Animals were sacrificed by decapitation 7 days after the injection, their striata were rapidly dissected out and frozen at −80°C, and Complexes I–IV were measured biochemically as described above. In the same tissue, glutamate decarboxylase (GAD) activity was determined as a measure of neuronal loss (64). Animals showing a less than 60% reduction in striatal GAD activity were not considered for analysis.

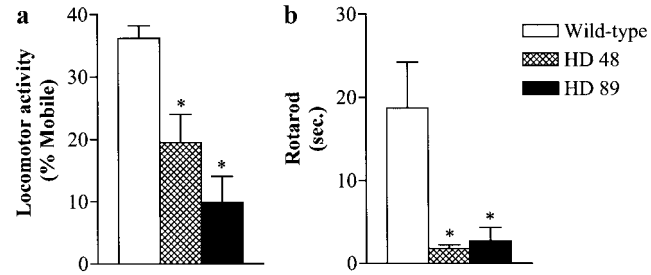

FIG. 1. Quantification of (a) locomotor activity and (b) Rotarod behavior in 13- to 16-month-old mice. "% Mobile" signifies the percentage of the time spent in movement during a 5-min observation period. Data are the average of two measurements conducted 1 week apart. Rotarod data represent the average of the second and third of three trials. Data represent the mean ± SEM of the number of animals indicated in parentheses. *$P < 0.05$ vs wild-type (ANOVA followed by Fisher's multiple-comparison test).

Statistical Analyses

Analyses were performed by one-way ANOVA with Fisher's LSD comparison test or Student's *t* test using a computerized software package (Number Cruncher Statistical System, Kaysville, UT). ANOVA and Student's *t* test for the analysis of enzyme activities was performed on logarithmically transformed data.

RESULTS

Behavioral Analyses

In line with previous observations (55, 56), transgenic mice expressing mutant huntingtin showed a series of progressive behavioral abnormalities. Thus, animals first displayed feet clasping starting at 2–4 months of age. Hyperactive behavior (including circling, backflips, and excessive grooming) developed at 5–7 months of age and lasted 3–9 months. This was followed by a 4- to 6-week period of hypoactivity. During this latter stage, the animals were analyzed for the present study. Eventually, the mice would have developed akinesia and died 6–10 days later. In terminally ill animals, a 20–50% cell loss is seen in the striatum, the cerebral cortex, and, to a lesser extent, in the hippocampus and the thalamus (55, 56).

Quantitative behavioral assessments of the 13- to 16-month-old transgenic mutant mice used in this study showed a reduction in motor activity (Fig 1a).

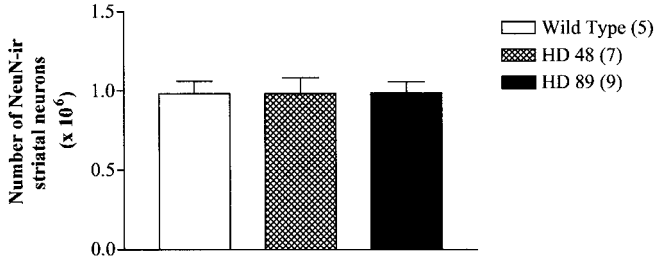

FIG. 2. Unbiased stereological estimation of NeuN-ir neurons in the caudate-putamen complex of phenotypically normal wild-type and hypoactive HD 48 and HD 89 transgenic mice. Data represent the mean ± SEM of the number of animals indicated in parentheses.

Compared to wild-type controls, both HD48 and HD89 transgenic animals spent less time roaming the activity chamber. The animals also had a substantial decline in motor coordination and balance since their performance on a Rotarod apparatus was decreased by over 85% (Fig 1b).

Stereological Cell Counts

Estimation of total striatal neuronal number was conducted to assess possible differences between hypoactive HD-transgenic mice (HD48, $n = 7$; HD89, $n = 9$) and age-matched wild-type controls ($n = 5$). Behaviorally tested hypoactive mice (Fig. 1a) showed no significant decrease in total number of NeuN-immunoreactive neurons within the striatum (Fig. 2), using unbiased stereological methods (73). Moreover no difference in striatal volume and neuronal density was detected in both HD48 and HD89 when compared to control animals.

Golgi Staining

To explore the possibility that neurons in these hypoactive mutant HD transgenic mice exhibit subtle morphological changes, striatal and cortical neuronal cytoarchitecture was examined in Golgi impregnated tissue. This method is commonly used to identify multipolar neurons, especially medium spiny neurons, in the striatum, and pyramidal projection neurons (layers 3, 5, and 6) in the cerebral cortex, i.e., cell types that are prominently affected in HD. Of note, Golgi studies in HD tissue have indicated both proliferative and degenerative dendritic changes in striatal spiny neurons, with the latter becoming more prominent in late-stage HD (17, 22).

Golgi staining of mutant HD transgenic mice revealed a prominent loss of primary dendritic spines in the striatum and a less pronounced but significant reduction in the cortex (Table 1). Moreover, a thickening of the proximal portion of primary dendrites was apparent in both striatal projection neurons and cortical neurons (Fig. 3d). Area measurements showed a significant decrease in the surface area of neuronal somata and dendrites, and these changes, too, were more obvious in the striatum than in the cortex. In addition, spines of the secondary dendrites of striatal spiny neurons showed an up to 40% decrease in density relative to controls (Table 1). Notably, very similar changes were observed in all these parameters in mutant mice containing 48 and 89 polyglutamine repeats.

Mitochondrial Enzymes in Transgenic HD Mice

Measurement of the enzymatic activities of Complexes I–IV demonstrated no significant differences between wild-type and HD48 or HD89 transgenics in either the striatum (Fig. 4b) or the sensorimotor cortex (Table 2).

Mitochondrial Enzymes in Human Neostriatum and Cortex

No linear correlation between enzyme activities and age or postmortem interval, respectively, was noted in striatal or cortical tissues of nine human control subjects ($P > 0.05$). Measurement of mitochondrial Complex I–IV activities in the neostriatum revealed significant reductions in the activities of Complex I (−42%), Complex II (−64%), Complex III

TABLE 1

Golgi Analysis of Mouse Striatum and Sensorimotor Cortex

	Striatum			Cortex		
	Wild-type	HD48	HD89	Wild-type	HD48	HD89
Total neuronal area (μm^2)	2893 ± 107	1439 ± 91*	1278 ± 97*	2117 ± 220	1571 ± 99*	1623 ± 73*
Dendritic area (μm^2)	405 ± 18	231 ± 18*	235 ± 21*	324 ± 16	191 ± 7*	207 ± 14*
1° Dendritic spines/20 μm	4.5 ± 0.7	0.5 ± 0.2*	0.1 ± 0.1*	3.2 ± 0.4	1.1 ± 0.3*	2.4 ± 0.6*
2° Dendritic spines/20 μm	10.5 ± 0.7	6.2 ± 0.5*	5.3 ± 0.4*	13.9 ± 0.6	11.1 ± 0.5*	11.0 ± 0.9

Note. Quantitative analysis of Golgi-impregnated striatal and cortical neurons was performed as described in the text. Data are the mean ± SEM of three wild-type mice, six HD48, and three HD89 transgenics. Results were obtained from 11–15 striatal and 5–15 cortical neurons per group.

* $P < 0.05$ vs wild-type (ANOVA followed by Fisher's multiple-comparison test).

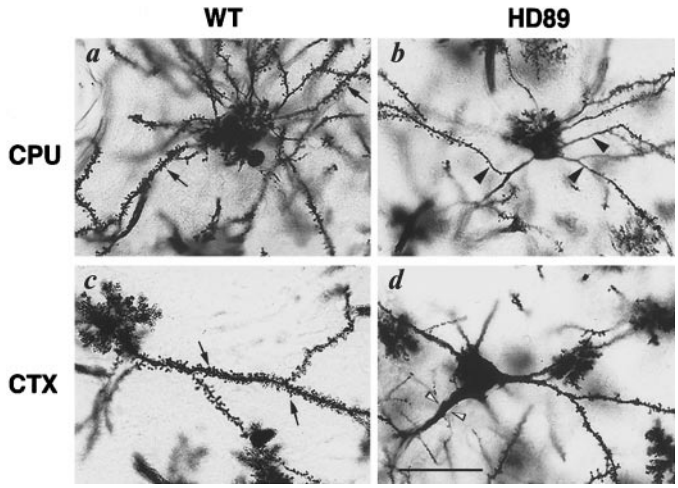

FIG. 3. Representative photomicrographs of Golgi-impregnated neurons from the caudate-putamen complex (CPU) and sensorimotor cortex (CTX) of a wild-type (WT) and a HD89 transgenic mutant mouse. (a) Wild-type striatum, (b) HD89 striatum; (c) wild-type frontal cortex; (d) HD89 frontal cortex. Compare the abundant dendritic spines along the length of the dendrites of the wild-type mouse with the dearth of spines and thickened proximal segments of the striatal and cortical dendrites in the mutant mouse. Arrows indicate spines, closed arrowheads show spine loss, and open arrowheads point to dendritic hypertrophy. All original magnification, 400×; bar, 50 μm.

(−50%), and Complex IV (−72%) in late-stage HD patients (grades 3/4) (Figs. 4a and 4b). In contrast, mitochondrial Complexes I–IV showed no significant decrements in the striatum of early HD cases (presymptomatic and grade 1) (Figs. 4a and 4b). Histochemical analysis of the putamen of grade 2 cases (n = 3) revealed a 20% decrease in Complex II and IV activities as compared to the putamen of controls (n = 4; data not shown). Thus, our results suggested a gradual decrease of mitochondrial enzyme activities which appeared to follow the progression of neuronal loss seen in HD (72).

Table 2 lists enzyme activities from the corresponding cerebral cortical samples. A significant reduction in Complex III was observed in late stage HD, but no other differences between controls, presymptomatic/grade 1 and grade 3/4 cases were found in the four mitochondrial enzyme activities.

Mitochondrial Enzymes in the Quinolinate-Lesioned Mouse Striatum

Since the reduction in the activity of Complexes I–IV in the striatum of late stage HD may be a consequence of extensive neuronal loss, striatal mitochondrial enzyme activities were determined biochemically in a separate group of 2-month-old FVB/N mice 1 week following a focal quinolinate injection. As detailed in Table 3, quinolinate-lesioned striata showed pronounced decrements in Complexes I–IV. Specifically, a 71 ± 4% reduction in GAD activity in the lesioned striatum was accompanied by 45–61% decreases in the activities of Complexes I–IV. Similar results were obtained in a group of animals injected with quinolinic acid and examined histochemically for Complexes I, II, and IV (n = 3; data not shown).

DISCUSSION

The results of the present study indicate that mutant huntingtin causes a behavioral phenotype and degenerative dendritic abnormalities in the absence of an impairment of the mitochondrial electron transfer chain. This conclusion is based on the study of (a) transgenic mutant HD mice, which had distinct behavioral abnormalities, showed no neuronal loss, and had normal activities of respiratory chain enzymes, and (b) presymptomatic and grade 1 HD brains, which presented with normal activities of the components of the mitochondrial electron transfer chain. In agreement with a number of previous studies (14, 15, 25, 68), we observed a loss of Complexes II, III, and IV in late-stage HD brains. Moreover, we found a decrease in striatal Complex I activity in these brains, which was similar in magnitude to that reported by Browne *et al.* (15), but reached statistical significance in our sample. The progressive decrease in Complex I–IV activities with increasing disease duration suggests that the reductions in late-stage HD brains are a result of pronounced neuronal loss. This was further supported in the present study following lesions in 2-month-old FVB/N wild-type mice. Thus, age-related decreases in basal enzyme activities not withstanding (75), an extensive striatal quinolinate lesion, which duplicates many characteristics of terminal HD (63), caused substantial decreases in all four mitochondrial complexes in these animals.

The present data need to be weighed against reports and hypotheses favoring early mitochondrial impairment as a principal pathogenic factor in HD. Clearly, experimentally induced mitochondrial dysfunction, effected by respiratory chain enzyme inhibitors such as 3-nitropropionic acid (9), malonate (10, 23), iodoacetate (76), or azide (35), results in NMDA receptor-mediated excitotoxicity. Dysregulation of mitochondrial energy production *can* therefore be the primary cause of neuronal loss and may indeed be critically involved in the early pathophysiology of neurodegenerative diseases (7, 8, 60). However, this cause–effect relationship does not appear to apply to HD, even though a CAG repeat length-dependent impairment of mitochondrial function is seen in muscle (5) and lymphoblasts (59) of HD patients.

If a dysfunctional mitochondrial respiratory chain is not a primary cause of HD pathology, other mech-

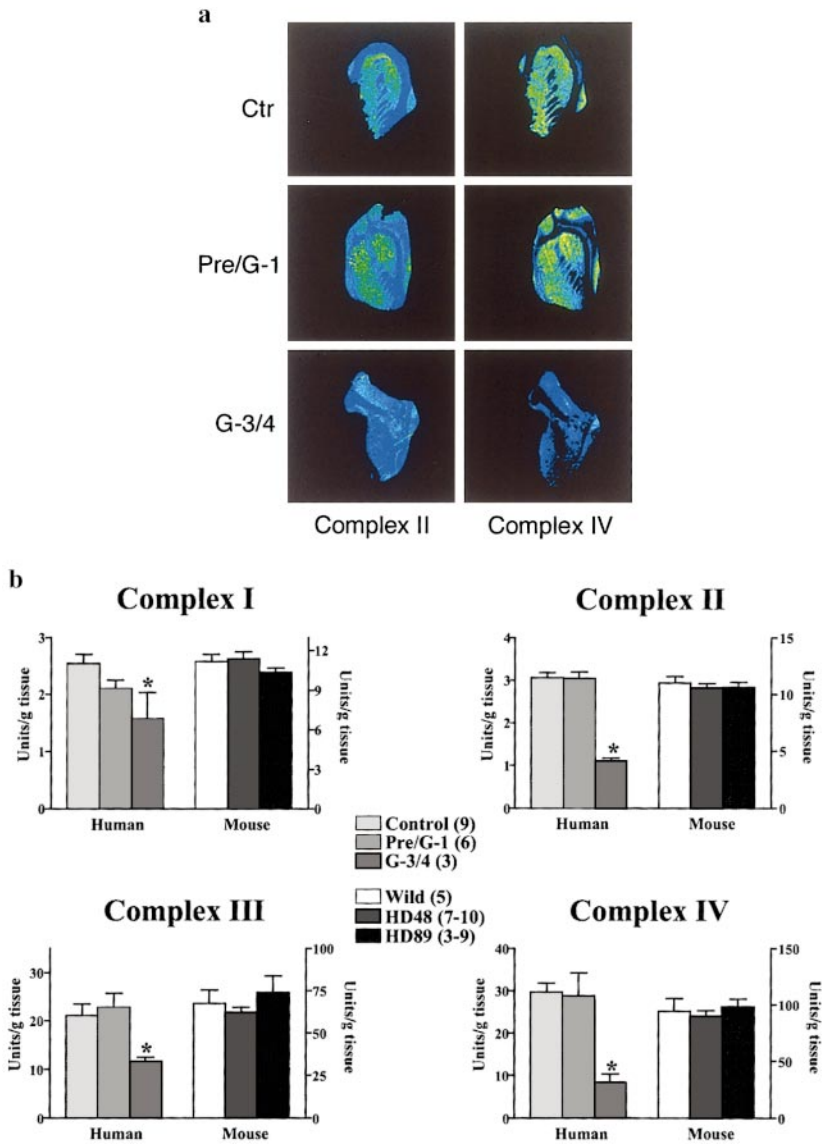

FIG. 4. Mitochondrial Complex I–IV activities in human and mouse. (a) Representative pseudo-color images of histochemical staining for Complex II and IV in human control, grade 1 HD and grade 4 HD tissue at the level of the caudate and putamen. (b) Quantification of the activity of Complexes I–IV in human neostriatum and mouse striatum. Data were obtained histochemically (Complexes I, II, and IV) or biochemically (Complex III) as described in the text and are the mean ± SEM of the number of subjects/animals indicated in parentheses. "Pre", presymptomatic for HD. "G-1" and "G-3/4" indicate HD grades. *$P < 0.05$ (ANOVA followed by Fisher's multiple-comparison test).

anisms must account for the metabolic changes and the associated reduction in basal ganglia volume which are seen in the early stages of HD. For example, the decrease in striatal glucose utilization (4, 11, 20, 21, 42, 48), creatine (58) and caudate size (20, 21, 28), and the elevated brain levels of lactate (36, 37, 40), which are detectable in presymptomatic gene carriers and grade 1 patients, might be a consequence of the early formation of large complexes between mutant huntingtin and other protein(s). These protein–protein interactions may involve binding of mutant huntingtin to the glycolytic enzyme glyceraldehyde phosphate dehydrogenase (16) or to proteins such as huntingtin-associated protein 1 (HAP-1), which is enriched in synaptic compartments and whose affinity for huntingtin is polyglutamine repeat length-dependent (26, 45, 50). These protein complexes, which appear to be promoted by HEAT repeats in the huntingtin protein (3), likely interfere not only with glycolysis but also with intracellular transport processes and synaptic vesicle trafficking and, thus, increase glutamatergic tone (6). Eventually, these abnormal cellular events can be envisioned to facilitate excitotoxic neuronal dam-

TABLE 2

Biochemical Assessment of Mitochondrial Complex Activities in the Sensorimotor Cortex

	Complex I	Complex II	Complex III	Complex IV
Transgenic mice				
Wild-type (5)	12.0 ± 0.9	12.0 ± 0.9	43.5 ± 5.6	85.2 ± 13.0
HD48 (7–10)	12.1 ± 0.4	12.1 ± 0.4	39.4 ± 4.3	85.0 ± 6.0
HD89 (3–9)	11.9 ± 0.4	11.9 ± 0.4	45.7 ± 6.8	92.2 ± 9.5
Humans				
Controls (9)	2.7 ± 0.1	2.4 ± 0.2	22.3 ± 2.5	35.1 ± 3.4
HD (Pre/G-1) (7)	2.3 ± 0.1	2.7 ± 0.2	28.7 ± 2.4	38.4 ± 4.1
HD (Grade 3/4) (3)	3.0 ± 0.2	1.9 ± 0.3	15.9 ± 2.4*	36.1 ± 1.8

Note. Data are expressed as units/g of tissue and represent the mean ± SEM of the number of animals or subjects listed in parentheses. See text for experimental details.

* $P < 0.05$ vs presymptomatic/grade 1 HD cases ("Pre/G-1") (ANOVA followed by Fisher's multiple-comparison test).

age. Notably, the high levels of lactate detected by MRI may reflect a glial reaction to increased glutamatergic function, since glia-derived lactate can be used by neurons as an efficient energy source (53, 62, 70) and is elevated in response to glutamate exposure (61).

The results from the present Golgi study are compatible with the idea that excitotoxic phenomena in HD occur prior to mitochondrial dysregulation and neuronal loss. Thus, 13- to 16-month-old mice transgenic for mutant huntingtin showed a substantial decrease in the density of dendritic spines, which are normally endowed with a large number of NMDA receptors (12). Our data suggest that the abnormal cellular events initiated by mutant huntingtin result in the excessive activation of these spinous NMDA receptors relatively early in the disease process and prior to significant neuronal loss. Through excitotoxic mechanisms, triggered by the enhanced influx and intracellular accumulation of Ca^{2+} (46), dendritic spines carrying NMDA receptors eventually degenerate. This loss of dendritic spines, rather than complete neuronal degeneration and cell loss, correlates with—and is conceivably the cause of—the distinct behavioral phenomena seen in mutant HD transgenic mice between 13 and 16 months of age, i.e., during their hypoactive stage. The comparatively less pronounced loss of dendritic spines in cortical neurons in these animals (cf. Table 1) suggests that the initial damage may occur in the striatum which is normally enriched with NMDA receptor-carrying medium spiny neurons (41). This primary insult would lead, in turn, to the progressive attenuation of cortico-striatal communication during the course of the disease.

The slow behavioral (hyperactive to hypoactive to akinetic stages) and the concomitant neurodegenerative progression renders the mutant HD transgenic mouse an excellent model for the study of cause–effect relationships between the primary genetic defect and subsequent pathological phenomena in HD. This model should therefore also prove useful for the exploration of therapeutic strategies. The present results suggest that the early treatment of HD should involve anti-excitotoxic interventions such as Ca^{2+} antagonists (33), free radical scavengers (52, 69), and compounds capable of decreasing glutamatergic transmission (38). At later stages of the disease, it may be equally or even more useful to target presumed downstream events of the neurodegenerative cascade, for example enzymes involved in apoptosis (49). Because of their ability to attenuate or prevent neuronal loss triggered by a variety of insults, energy replacement therapies using creatine (39), pyruvate (34, 47), or related agents may show therapeutic benefits at any stage of the disease.

TABLE 3

Biochemical Assessment of Striatal Mitochondrial Complex Activities in 2-Month-Old FVB/N Mice: Effects of Neuronal Loss

	Complex I	Complex II	Complex III	Complex IV
Contralateral striatum	17.4 ± 0.3	9.6 ± 0.2	87.4 ± 2.0	195.6 ± 4.6
Lesioned striatum	9.6 ± 0.4*	3.1 ± 0.1*	38.8 ± 2.1*	75.8 ± 6.5*

Note. Animals were killed 7 days after a unilateral intrastriatal quinolinic acid injection (60 nmol/0.5 μl). Results are expressed as units/g of tissue and represent the mean ± SEM of five animals.

* $P < 0.05$ vs the contralateral side (paired Student's test).

ACKNOWLEDGMENTS

We thank Dr. Francis S. Collins for critical reading of the manuscript, and Tracie Moss for technical support. Human tissues were provided by the Harvard Brain Tissue Resource Center, which is supported in part by PHS Grant MH/NS 31862. V.C. received a PRAT fellowship from NIGMS, and P.H.R. was the recipient of a Fellowship from the Huntington's Disease Society of America, Inc. This work was supported in part by PHS Grant NS 28236 to R.S. and W.O.W. and by a grant from the Cure HD Initiative–Hereditary Disease Foundation to D.A.T.

REFERENCES

1. Ackrell, B. A., E. B. Kearney, and T. P. Singer. 1978. Mammalian succinate dehydrogenase. *Methods Enzymol.* **53:** 466–483.
2. Alexi, T., P. E. Hughes, B. Knusel, and A. J. Tobin. 1998. Metabolic compromise with systemic 3-nitropropionic acid produces striatal apoptosis in Sprague–Dawley rats but not in BALB/c ByJ mice. *Exp. Neurol.* **153:** 74–93.
3. Andrade, M. A., and P. Bork. 1995. HEAT repeats in the Huntington's disease protein. *Nat. Genet.* **11:** 115–116.
4. Antonini, A., K. Leenders, R. Spiegel, D. Meier, P. Vontobel, M. Weigell-Weber, R. Sanchez-Pernaute, J. De Yebenez, P. Boesiger, A. Weindl, and R. Maguire. 1996. Striatal glucose metabolism and dopamine D2 receptor binding in asymptomatic gene carriers and patients with Huntington's disease. *Brain* **119:** 2085–2095.
5. Arenas, J., Y. Campos, R. Ribacoba, M. A. Martin, J. C. Rubio , P. Ablanedo, and O. A. Cabell. 1998. Complex I defect in muscle from patients with Huntington's disease. *Ann. Neurol.* **43:** 397–400.
6. Aronin, N., M. Kim, G. Laforet, and M. DiFiglia. 1999. Are there multiple pathways in the pathogenesis of Huntington's disease? *Philos. Trans. R. Soc. London B* **354:** 995–1003.
7. Beal, M. F. 1993. Do defects in mitochondrial energy metabolism underlie the pathology of neurodegenerative diseases? *Trends Neurosci.* **16:** 125–131.
8. Beal, M. F. 1998. Mitochondrial dysfunction in neurodegenerative diseases. *Biochim. Biophys. Acta* **1366:** 211–223.
9. Beal, M. F., E. Brouillet, B. G. Jenkins, R. J. Ferrante, N. W. Kowall, J. M. Miller, E. Storey, R. Srivastava, B. R. Rosen, and B. T. Hyman. 1993. Neurochemical and histologic characterization of striatal excitotoxic lesions produced by the mitochondrial toxin 3-nitropropionic acid. *J. Neurosci.* **13:** 4181–4192.
10. Beal, M. F., E. Brouillet, B. G. Jenkins, R. Henshaw, B. Rosen, and B. T. Hyman. 1993. Age-dependent striatal excitotoxic lesions produced by the endogenous mitochondrial inhibitor malonate. *J. Neurochem.* **61:** 1147–1150.
11. Berent, S., B. Giordani, S. Lehtinen, D. Markel, J. B. Penney, H. A. Buchtel, S. Starosta-Rubinstein, R. Hichwa, and A. B. Young. 1988. Positron emission tomographic scan investigations of Huntington's disease: Cerebral metabolic correlates of cognitive function. *Ann. Neurol.* **23:** 541–546.
12. Bernard, V., and J. Bolam. 1998. Subcellular and subsynaptic distribution of the NR1 subunit of the NMDA receptor in the neostriatum and globus pallidus of the rat: Co-localization at synapses with the GluR2/3 subunit of the AMPA receptor. *Eur. J. Neurosci.* **10:** 3721–3736.
13. Bowling, A. C., and M. F. Beal. 1995. Bioenergetic and oxidative stress in neurodegenerative diseases. *Life Sci.* **56:** 1151–1171.
14. Brennan, W. A., Jr., E. D. Bird, and J. R. Aprille. 1985. Regional mitochondrial respiratory activity in Huntington's disease brain. *J. Neurochem.* **44:** 1948–1950.
15. Browne, S. E., A. C. Bowling, U. Macgarvey, M. J. Baik, S. C. Berger, M. M. Muqit, E. D. Bird, and M. F. Beal. 1997. Oxidative damage and metabolic dysfunction in Huntington's disease: Selective vulnerability of the basal ganglia. *Ann. Neurol.* **41:** 646–653.
16. Burke, J. R., J. J. Enghild, M. E. Martin, Y. S. Jou, R. M. Myers, A. D. Roses, J. M. Vance, and W. J. Strittmatter. 1996. Huntingtin and DRPLA proteins selectively interact with the enzyme GAPDH. *Nat. Med.* **2:** 347–350.
17. Ferrante, R. J., N. W. Kowall, and E. P. Richardson, Jr. 1991. Proliferative and degenerative changes in striatal spiny neurons in Huntington's disease: A combined study using the section-Golgi method and calbindin D28k immunocytochemistry. *J. Neurosci.* **11:** 3877–3887.
18. Folstein, S. E. 1990. *Huntington's Disease.* The Johns Hopkins University Press, Baltimore.
19. Gonzalez-Lima, F., and M. Garrosa. 1991. Quantitative histochemistry of cytochrome oxidase in rat brain. *Neurosci. Lett.* **123:** 251–253.
20. Grafton, S., J. Mazziotta, J. Pahl, P. St. George-Hyslop, J. Haines, J. Gusella, J. Hoffman, L. Baxter, and M. Phelps. 1990. A comparison of neurological, metabolic, structural, and genetic evaluations in persons at risk for Huntington's disease. *Ann. Neurol.* **28:** 614–621.
21. Grafton, S. T., J. C. Mazziotta, J. J. Pahl, P. St. George-Hyslop, J. L. Haines, J. Gusella, J. M. Hoffman, L. R. Baxter, and M. E. Phelps. 1992. Serial changes of cerebral glucose metabolism and caudate size in persons at risk for Huntington's disease. *Arch. Neurol.* **49:** 1161–1167.
22. Graveland, G. A., R. S. Williams, and M. DiFiglia. 1985. Evidence for degenerative and regenerative changes in neostriatal spiny neurons in Huntington's disease. *Science* **227:** 770–773.
23. Greene, J. G., and J. T. Greenamyre. 1995. Exacerbation of NMDA, AMPA, and L-glutamate excitotoxicity by the succinate dehydrogenase inhibitor malonate. *J. Neurochem.* **64:** 2332–2338.
24. Greene, J. G., and J. T. Greenamyre. 1996. Bioenergetics and glutamate excitotoxicity. *Prog. Neurobiol.* **48:** 613–634.
25. Gu, M., M. T. Gash, V. M. Mann, F. Javoy-Agid, J. M. Cooper, and A. H. Schapira. 1996. Mitochondrial defect in Huntington's disease caudate nucleus. *Ann. Neurol.* **39:** 385–389.
26. Gutekunst, C. A., S. H. Li, H. Yi, R. J. Ferrante, X. J. Li, and S. M. Hersch. 1998. The cellular and subcellular localization of huntingtin-associated protein 1 (HAP1): Comparison with huntingtin in rat and human. *J. Neurosci.* **18:** 7674–7686.
27. Halkjaer-Kristensen, J., and T. Ingemann-Hansen. 1979. Microphotometric analysis of NADH-tetrazolium reductase and alpha-glycerophosphate dehydrogenase in human quadriceps muscle. *Histochem. J.* **11:** 127–136.
28. Harris, G. J., A. M. Codori, R. F. Lewis, E. Schmidt, A. Bedi, and J. Brandt. 1999. Reduced basal ganglia blood flow and volume in pre-symptomatic, gene-tested persons at-risk for Huntington's disease. *Brain* **122:** 1667–1678.
29. Hatefi, Y. 1978. Preparation and properties of dihydroubiquinone: cytochrome c oxidoreductase (complex III). *Methods Enzymol.* **53:** 35–40.
30. Hatefi, Y. 1978. Preparation and properties of NADH: Ubiquinone oxidoreductase (complex I), EC 1.6.5.3. *Methods Enzymol.* **53:** 11–14.
31. The Huntington's Disease Collaborative Research Group. 1993. A novel gene containing a trinucleotide repeat that is expanded and unstable on Huntington's disease chromosomes. *Cell* **72:** 971–983.

32. Hess, H. H., and A. Pope. 1953. Ultramicrospectrophotomeric determination of cytochrome oxidase for quantitative histochemistry. *J. Biol. Chem.* **204:** 296–306.
33. Hyrc, K., S. Handran, S. Rothman, and M. Goldberg. 1997. Ionized intracellular calcium concentration predicts excitotoxic neuronal death: Observations with low-affinity fluorescenct calcium indicators. *J. Neurosci.* **17:** 6669–6677.
34. Izumi, Y., A. Benz, H. Katsuki, and C. Zorumski. 1997. Endogenous monocarboxylates sustain hippocampal synaptic function and morphological integrity during energy deprivation. *J. Neurosci.* **17:** 9448–9457.
35. Jenkins, B. G., E. Brouillet, Y. C. Chen, E. Storey, J. B. Schulz, P. Kirschner, M. F. Beal, and B. R. Rosen. 1996. Non-invasive neurochemical analysis of focal excitotoxic lesions in models of neurodegenerative illness using spectroscopic imaging. *J. Cereb. Blood Flow Metab.* **16:** 450–461.
36. Jenkins, B. G., W. J. Koroshetz, M. F. Beal, and B. R. Rosen. 1993. Evidence for impairment of energy metabolism in vivo in Huntington's disease using localized 1H NMR spectroscopy. *Neurology* **43:** 2689–2695.
37. Jenkins, B. G., H. D. Rosas, Y. C. Chen, T. Makabe, R. Myers, M. Macdonald, B. R. Rosen, M. F. Beal, and W. J. Koroshetz. 1998. 1H NMR spectroscopy studies of Huntington's disease: Correlations with CAG repeat numbers. *Neurology* **50:** 1357–1365.
38. Kieburtz, K. 1999. Antiglutamate therapies in Huntington's disease. *J. Neural Transm. Suppl.* **55:** 97–102.
39. Klivenyi, P., R. Ferrante, R. Matthews, M. Bogdanov, A. Klein, O. Andreassen, G. Mueller, M. Wermer, R. Kaddurah-Daouk, and M. F. Beal. 1999. Neuroprotective effects of creatine in a transgenic animal model of amyotrophic lateral sclerosis. *Nat. Med.* **5:** 347–350.
40. Koroshetz, W. J., B. G. Jenkins, B. R. Rosen, and M. F. Beal. 1997. Energy metabolism defects in Huntington's disease and effects of coenzyme Q10. *Ann. Neurol.* **41:** 160–165.
41. Kuppenbender, K., D. Standaert, T. Feuerstein, J. J. Penney, A. Young, and G. Landwehrmeyer. 2000. Expression of NMDA receptor subunit mRNAs in neurochemically identified projection and interneurons in the human striatum. *J. Comp. Neurol.* **419:** 407–421.
42. Kuwert, T., H. W. Lange, H. Boecker, H. Titz, H. Herzog, A. Aulich, B. C. Wang, U. Nayak, and L. E. Feinendegen. 1993. Striatal glucose consumption in chorea-free subjects at risk of Huntington's disease *J. Neurol.* **241:** 31–36.
43. Landas, S., and M. I. Phillips. 1982. Staining of human and rat brain Vibratome sections by a new Golgi method. *J. Neurosci. Methods* **5:** 147–151.
44. Li, S. H., G. Schilling, W. S. D. Young, X. J. Li, R. L. Margolis, O. C. Stine, M. V. Wagster, M. H. Abbott, M. L. Franz, N. G. Ranen, S. E. Folstein, J. C. Hedreen, and C. A. Ross. 1993. Huntington's disease gene (IT15) is widely expressed in human and rat tissues. *Neuron* **11:** 985–993.
45. Li, X. J., S. H. Li, A. H. Sharp, F. C. Nucifora, Jr., G. Schilling, A. Lanahan, P. Worley, S. H. Snyder, and C. A. Ross. 1995. A huntingtin-associated protein enriched in brain with implications for pathology. *Nature* **378:** 398–402.
46. Lipton, S. A. 1991. Calcium channel antagonists in the prevention of neurotoxicity. *Adv. Pharmacol.* **22:** 271–297.
47. Maus, M., P. Marin, M. Israel, J. Glowinski, and J. Premont. 1999. Pyruvate and lactate protect striatal neurons against N-methyl-D-aspartate-induced neurotoxicity. *Eur. J. Neurosci.* **11:** 3215–3224.
48. Mazziotta, J., M. Phelps, J. Pahl, S. Huang, L. Baxter, W. Riege, J. Hoffman, D. Kuhl, A. Lanto, and W. Ja. 1987. Reduced cerebral glucose metabolism in asymptomatic subjects at risk for Huntington's disease. *N. Engl. J. Med.* **316:** 357–362.
49. Ona, V. O., M. Li, J. P. Vonsattel, L. J. Andrews, S. Q. Khan, W. M. Chung, A. S. Frey, A. S. Menon, X. J. Li, P. E. Stieg, J. Yuan, J. B. Penney, A. B. Young, J. H. Cha, and R. M. Friedlander. 1999. Inhibition of caspase-1 slows disease progression in a mouse model of Huntington's disease. *Nature* **399:** 263–267.
50. Page, K. J., L. Potter, S. Aronni, B. J. Everitt, and S. B. Dunnett. 1998. The expression of Huntingtin-associated protein (HAP1) mRNA in developing, adult and ageing rat CNS: Implications for Huntington's disease neuropathology. *Eur. J. Neurosci.* **10:** 1835–1845.
51. Parker, W. D., S. J. Boyson, A. S. Luder, and J. K. Parks. 1990. Evidence for a defect in NADH: Ubiquinone oxidoreductase (complex I) in Huntington's disease. *Neurology* **40:** 1231–1234.
52. Patel, M., B. J. Day, J. D. Crapo, I. Fridovich, and J. O. McNamara. 1996. Requirement for superoxide in excitotoxic cell death. *Neuron* **16:** 345–355.
53. Pellerin, L., and P. Magistretti. 1994. Glutamate uptake into astrocytes stimulates aerobic glycolysis: A mechanism coupling neuronal activity to glucose utilization. *Proc. Natl. Acad. Sci. USA* **91:** 10625–10629.
54. Poeggeler, B., A. Rassoulpour, P. Guidetti, H. Q. Wu, and R. Schwarcz. 1998. Dopaminergic control of kynurenate levels and N-methyl-D-aspartate toxicity in the developing rat striatum. *Dev. Neurosci.* **20:** 146–153.
55. Reddy, P. H., V. Charles, M. Williams, G. Miller, W. O. Whetsell, Jr., and D. A. Tagle. 1999. Transgenic mice expressing mutated full-length HD cDNA: A paradigm for locomotor changes and selective neuronal loss in Huntington's disease. *Philos Trans. R. Soc. London B* **354:** 1035–1045.
56. Reddy, P. H., M. Williams, V. Charles, L. Garrett, L. Pike-Buchanan, W. O. Whetsell, Jr., G. Miller, and D. A. Tagle. 1998. Behavioural abnormalities and selective neuronal loss in HD transgenic mice expressing mutated full-length HD cDNA. *Nat. Genet.* **20:** 198–202.
57. Reddy, P. H., M. Williams, and D. A. Tagle. 1999. Recent advances in understanding the pathogenesis of Huntington's disease. *Trends Neurosci.* **22:** 248–255.
58. Sanchez-Pernaute, R., J. Garcia-Segura, A. Del Barrio Alba, J. Viano, and J. De Yebenes. 1999. Clinical correlation of striatal 1H MRS changes in Huntington's disease. *Neurology* **53:** 806–812.
59. Sawa, A., G. Wiegand, J. Cooper, R. Margolis, A. Sharp, J. J. Lawler, J. Greenamyre, S. H. Snyder, and C. Ross. 1999. Increased apoptosis of Huntington disease lymphoblasts associated with repeat length-dependent mitochondrial depolarization. *Nat. Med.* **5:** 1194–1198.
60. Schapira, A. H. 1998. Mitochondrial dysfunction in neurodegenerative disorders. *Biochim. Biophys. Acta* **1366:** 225–233.
61. Schurr, A., J. J. Miller, R. S. Payne, and B. M. Rigor. 1999. An increase in lactate output by brain tissue serves to meet the energy needs of glutamate-activated neurons. *J. Neurosci.* **19:** 34–39.
62. Schurr, A., R. Payne, J. Miller, and B. Rigor. 1997. Glia are the main source of lactate utilized by neurons for recovery of function posthypoxia. *Brain Res.* **4:** 221–224.
63. Schwarcz, R., and I. Shoulson. 1987. Excitotoxins and Huntington's disease. In *Animal Models of Dementia: A Synaptic Neurochemical Perspective* (Coyle, J. T., Ed.), pp. 39–68. A. R. Liss, New York.
64. Schwarcz, R., W. O. Whetsell, Jr., and R. M. Mangano. 1983. Quinolinic acid: An endogenous metabolite that produces axon-sparing lesions in rat brain. *Science* **219:** 316–318.
65. Sharp, A. H., S. J. Loev, G. Schilling, S. H. Li, X. J. Li, J. Bao, M. V. Wagster, J. A. Kotzuk, J. P. Steiner, A. Lo, J. Hedreen, S.

Sisodia, S. H. Snyder, T. M. Dawson, D. K. Ryugo and C. A. Ross. 1995. Widespread expression of Huntington's disease gene (IT15) protein product. *Neuron* **14:** 1065–1074.

66. Soltanpour, N., D. M. Baker, and R. M. Santer. 1996. Neurons and microvessels of the nodose (vagal sensory) ganglion in young adult and aged rats: Morphometric and enzyme histochemical studies. *Tissue Cell* **28:**593–602.
67. Strong, T. V., D. A. Tagle, J. M. Valdes, L. W. Elmer, K. Boehm, M. Swaroop, K. W. Kaatz, F. S. Collins, and R. L. Albin. 1993. Widespread expression of the human and rat Huntington's disease gene in brain and nonneural tissues. *Nat. Genet.* **5:** 259–265.
68. Tabrizi, S. J., M. W. Cleeter, J. Xuereb, J. W. Taanman, J. M. Cooper, and A. H. Schapira. 1999. Biochemical abnormalities and excitotoxicity in Huntington's disease brain. *Ann. Neurol.* **45:** 25–32.
69. Tabrizi, S. J., J. Workman, P. E. Hart, L. Mangiarini, A. Mahal, G. Bates, J. M. Cooper, and A. H. Schapira. 2000. Mitochondrial dysfunction and free radical damage in the Huntington R6/2 transgenic mouse. *Ann. Neurol.* **47:** 80–86.
70. Tsacopoulos, M., and P. Magistretti. 1996. Metabolic coupling between glia and neurons. *Neurosci. Lett.* **16:** 877–885.
71. Valdes, J. M., D. A. Tagle, L. W. Elmer, and F. S. Collins. 1993. A simple non-radioactive method for diagnosis of Huntington's disease. *Hum. Mol. Genet.* **2:** 633–634.
72. Vonsattel, J. P., R. H. Myers, T. J. Stevens, R. J. Ferrante, E. D. Bird, and E. P. Richardson, Jr. 1985. Neuropathological classification of Huntington's disease. *J. Neuropathol. Exp. Neurol.* **44:** 559–577.
73. West, M. J. 1993. New stereological methods for counting neurons. *Neurobiol. Aging* **14:** 275–285.
74. West, M. J., L. Slomianka, and H. J. Gundersen. 1991. Unbiased stereological estimation of the total number of neurons in thesubdivisions of the rat hippocampus using the optical fractionator. *Anat. Rec.* **231:** 482–497.
75. Wong-Riley, M. T. 1989. Cytochrome oxidase: an endogenous metabolic marker for neuronal activity. *Trends Neurosci.* **12:** 94–101.
76. Zeevalk, G. D., and W. J. Nicklas. 1991. Mechanisms underlying initiation of excitotoxicity associated with metabolic inhibition. *J. Pharmacol. Exp. Ther.* **257:** 870–878.
77. Zeevalk, G. D., and W. J. Nicklas. 1993. Hypothermia, metabolic stress, and NMDA-mediated excitotoxicity. *J. Neurochem.* **61:** 1445–1153.